BIOCHEMISTRY
including biophysical chemistry & molecular biology

Article

pubs.acs.org/biochemistry

Mechanistic and Computational Studies of the Reductive Half-Reaction of Tyrosine to Phenylalanine Active Site Variants of D-Arginine Dehydrogenase

Swathi Gannavaram,[†] Sarah Sirin,[⊥] Woody Sherman,[⊥] and Giovanni Gadda*[,†,‡,§,∥]

Departments of [†]Chemistry and [‡]Biology, [§]Center for Biotechnology and Drug Design, and [∥]Center for Diagnostics and Therapeutics, Georgia State University, Atlanta, Georgia 30302-3965, United States

[⊥]Schrödinger, LLC, 120 West 45st Street, New York, New York 10036, United States

ABSTRACT: The flavin-mediated enzymatic oxidation of a CN bond in amino acids can occur through hydride transfer, carbanion, or polar nucleophilic mechanisms. Previous results with D-arginine dehydrogenase from *Pseudomonas aeruginosa* (PaDADH) using multiple deuterium kinetic isotope effects (KIEs) and computational studies established preferred binding of the substrate protonated on the α-amino group, with cleavages of the NH and CH bonds occurring in asynchronous fashion, consistent with the three possible mechanisms. The hydroxyl groups of Y53 and Y249 are ≤4 Å from the imino and carboxylate groups of the reaction product iminoarginine, suggesting participation in binding and catalysis. In this study, we have investigated the reductive half-reactions of the Y53F and Y249F variants of PaDADH using substrate and solvent deuterium KIEs, solvent viscosity and pH effects, and quantum mechanical/molecular mechanical computational approaches to gain insights into the catalytic roles of the tyrosines and evaluate whether their mutations affect the transition state for substrate oxidation. Both Y53F and Y249F enzymes oxidized D-arginine with steady-state kinetic parameters similar to those of the wild-type enzyme. Rate constants for flavin reduction (k_{red}) with D-leucine, a slow substrate amenable to rapid kinetics, were 3-fold smaller than the wild-type value with similar pK_a values for an unprotonated group of ~10.0. Similar pK_a values were observed for $^{app}K_d$ in the variant and wild-type enzymes. However, cleavage of the substrate NH and CH bonds in the enzyme variants occurred in synchronous fashion, as suggested by multiple deuterium KIEs on k_{red}. These data can be reconciled with a hydride transfer mechanism, but not with carbanion and polar nucleophilic mechanisms.

Pseudomonas aeruginosa D-arginine dehydrogenase (PaDADH) is a member of a structural family consisting of D-amino acid oxidase, sarcosine oxidase, dimethyl glycine oxidase, and glycine oxidase.[1−7] The enzyme, along with L-arginine dehydrogenase (PaLADH), is part of a recently discovered, two-enzyme system involved in D- to L-arginine racemization in pseudomonads and related species (Scheme 1).[8,9] Prior to this discovery, racemization between D- and L-amino acids was known to be catalyzed only by single PLP-dependent or -independent racemases.[10] PaDADH is a FAD-dependent enzyme that oxidizes D-arginine to iminoarginine, which is then hydrolyzed nonenzymatically to 2-ketoarginine and ammonia (Scheme 1A).[8] The latter compounds are substrates for the NAD(P)H-dependent PaLADH for the synthesis of L-arginine (Scheme 1B). L-Arginine is shuttled through different pathways to yield physiologically important compounds in bacteria[11] as well as mammals[12] (Scheme 1B). Although PaDADH is primarily involved in arginine metabolism in *P. aeruginosa*, the enzyme has broad substrate specificity for D-amino acids except D-aspartate, D-glutamate, and glycine.[9]

Scheme 1. Illustration of D- to L-Arginine Racemization in *P. aeruginosa* and Possible Fates of L-Arginine

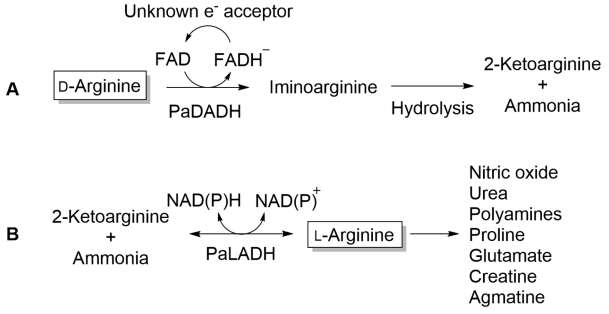

The FAD-mediated oxidation of the CN bond in PaDADH was recently investigated with D-leucine, a catalytically slow substrate for the enzyme.[13] With arginine, mechanistic analysis is precluded because >85% of the reaction happens within the mixing time of the stopped-flow spectrophotometer (i.e., 2.2 ms).[14] Deuterium kinetic isotope effects (KIE) and solvent effects (isotope, pH, and viscosity) in combination with molecular dynamics simulations are consistent with preferred

Received: July 25, 2014
Published: September 22, 2014

   dx.doi.org/10.1021/bi500917q | *Biochemistry* 2014, 53, 6574−6583

Scheme 2. Possible Mechanisms for CN Bond Oxidation by PaDADH, Carbanion (a–c), Hydride Transfer (d and e), and Polar Nucleophilic Attack (f–h)

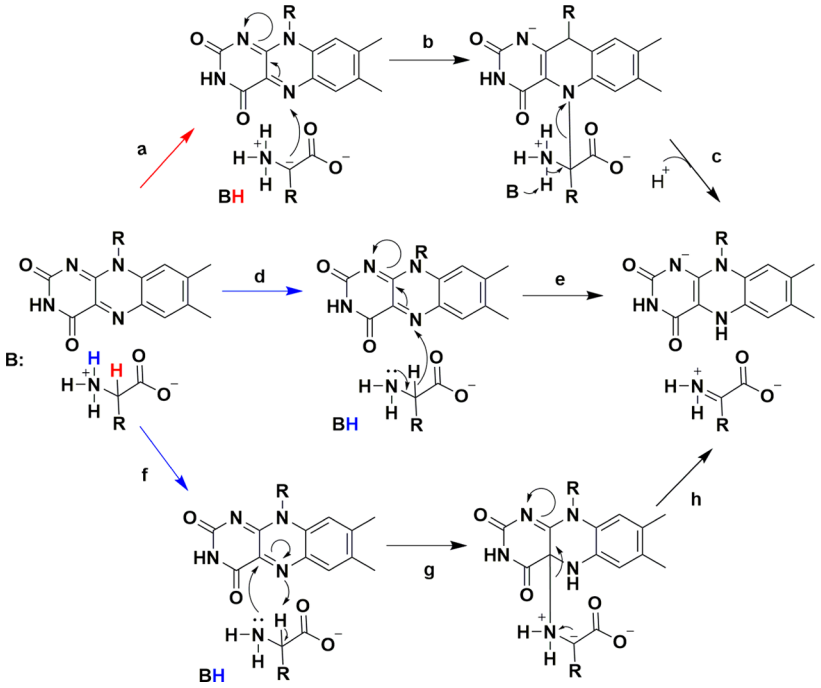

binding to the enzyme of D-leucine protonated on the α-amino group.[13] Multiple deuterium KIEs on the rate constant for flavin reduction (k_{red}) established that cleavages of the NH and CH bonds occur in asynchronous fashion. Three mechanisms for CN bond oxidation are consistent with the available data.

If a strong active site base abstracts the substrate α-proton with a pK_a of ~17,[15] the resulting carbanion would react with the flavin N5 atom forming a covalent N5-flavin adduct (Scheme 2, a–c).[1,16−20] Alternatively, a polar nucleophilic attack of the lone pair of electrons of the substrate α-amine at the flavin C4a atom may form a covalent C4a-flavin adduct (Scheme 2, f–h).[21] In both mechanisms, cleavage of the substrate NH bond would occur stepwise with respect to CH bond cleavage, either before (f) or after (c) formation of a covalent adduct with the flavin. If deprotonation of the substrate α-amine occurs first, it would trigger CH bond cleavage through the transfer of a hydride ion from the substrate to the flavin N5 atom (Scheme 2, d and e). While in principle the transfer of a single electron and a hydrogen atom from the substrate to the flavin is possible, mechanistic studies have yet to demonstrate in flavoproteins the transient existence of the resulting radical species in reactions with physiological substrates.

During reduction of PaDADH with D-leucine[13] or D-histidine,[14] no reaction intermediates characteristic of flavin C4a and N5 adducts, i.e., with absorbance maxima in the range of 360–400 nm, were reported, consistent with a hydride transfer mechanism. However, carbanion and polar nucleophilic mechanisms could not be ruled out solely on the basis of these observations because flavin adducts that decay faster than they form would not accumulate.

Steady-state and rapid kinetics pH profiles with D-leucine demonstrated in PaDADH the requirement for catalysis of an unprotonated group with a pK_a of 9.6.[13,22] A protonated group with a pK_a of ~10.3 favors the binding of the substrate to the enzyme.[13] X-ray crystallography of the enzyme in complex with iminoarginine or iminohistidine showed that Y53 is suitably positioned in the active site to deprotonate the substrate α-amine,[13,22] being on a mobile loop with its hydroxyl oxygen atom ≤3.8 Å from the imine of iminoarginine (Figure 1). The

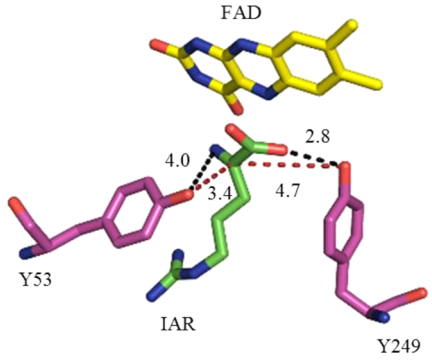

Figure 1. Active site of PaDADH in complex with iminoarginine at 1.3 Å resolution (Protein Data Bank entry 3NYE). The distances in angstroms from the hydroxyl oxygen atom of Y53 or Y249 to the imine nitrogen atom or carboxylate oxygen atom of the reaction product are shown in black, whereas those to the C_α atom are shown in red. IAR is iminoarginine.

side chain of Y249 interacts with the product carboxylate at a distance of ~2.8 Å, suggesting that Y249 may be the protonated group that facilitates substrate binding (Figure 1).

In this study, we have replaced Y53 and Y249 with phenylalanine to investigate the roles of their hydroxyl groups in catalysis and binding in PaDADH and gain insights into the relative timing of CH and NH bond cleavage in the enzyme variants. To this end, we used steady-state and rapid reaction kinetics, pH and solvent effects, deuterium substrate, solvent and multiple KIEs, and quantum mechanical/molecular mechanical (QM/MM) computational approaches. The results presented are consistent with a hydride transfer mechanism for

dx.doi.org/10.1021/bi500917q | Biochemistry 2014, 53, 6574–6583

amino acid oxidation in the enzyme variants lacking protein hydroxyls in the active site, but not with carbanion and polar nucleophilic mechanisms of catalysis.

EXPERIMENTAL PROCEDURES

Materials. *Escherichia coli* Rosetta(DE3)pLysS was from Novagen (Madison, WI). The QIAprep Spin Miniprep kit was obtained from Qiagen (Valencia, CA), and the QuickChange site-directed mutagenesis kit was purchased from Stratagene (La Jolla, CA). Oligonucleotides for site-directed mutagenesis and sequencing of the mutant genes were obtained from Sigma Genosys (The Woodlands, TX). D-Arginine and phenazine methosulfate (PMS) were purchased from Sigma-Aldrich (St. Louis, MO). D-Leucine was obtained from Alfa Aesar, and D-leucine-d_{10} was obtained from CDN isotopes. Deuterium oxide (99.9%) was purchased from Cambridge Isotope Laboratories, Inc. (Andover, MA). All other reagents used were obtained at the highest purity commercially available.

Site-Directed Mutagenesis, Expression, and Purification of the Y53F and Y249F Enzymes. The Y53F and Y249F enzymes were prepared by site-directed mutagenesis using the cloned wild-type gene pET20b(+)/PA3863 as a template. Site-directed mutagenesis was performed as per the manufacturer's instructions using the QuickChange kit. Dimethyl sulfoxide was added at a final concentration of 5% to ensure proper separation of the double-stranded DNA template. Each mutation was confirmed through sequencing the gene using an Applied Biosystems Big Dye Kit on an Applied Biosystems model ABI377 DNA sequencer, at the DNA Core Facility of Georgia State University. Rosetta(DE3)pLysS cells were transformed via heat shock. All steps of protein expression and purification were conducted at 4 °C using the published protocol for the wild-type enzyme.[14]

Steady-State Kinetics. Steady-state kinetic parameters with D-arginine (0.01−3.0 mM) were determined by measuring initial rates of reaction with an oxygen electrode in the presence of 1 mM PMS (K_m = 10 μM) as an electron acceptor in 20 mM Tris-HCl, at pH 8.7 and 25 °C, as previously described.[14] As for the wild-type enzyme, both Y53F and Y249F enzymes showed no oxygen consumption in absence of PMS, indicating that the mutations did not confer oxidase activity to the enzyme.

Reductive Half-Reaction. Reductive half-reactions were conducted using an SF-61DX2 Hi-Tech KinetAsyst high-performance stopped-flow spectrophotometer at 25 °C. For substrate, solvent, and multiple deuterium KIE as well as pH and solvent viscosity effects, the published protocols and buffers previously used for the wild-type enzyme were employed.[13] Final concentrations of D-leucine and enzyme were 0.1−50 mM and ∼10 μM to ensure pseudo-first-order kinetic conditions. Deuterium KIEs were determined in 20 mM EDTA, at pL 10.5 and 25 °C, in either H_2O or 99.9% D_2O with D-leucine and D-leucine-d_{10} as substrates, as previously described for the wild-type enzyme.[13]

Computational Characterization. Computational models of the reactant were prepared on the basis of the wild-type crystal structures of PaDADH (Protein Data Bank entries 3NYC and 3NYE).[22] To model the open, substrate free configuration of PaDADH, 3NYC was used, which corresponds to 70% occupancy of the ligand free open conformer.[22] The Y53 side chain rotamer corresponding to the open configuration was modeled after removing the imino product. For all other amino acids with multiple rotamers, side chains with higher occupancies were used. For the closed, substrate-bound PaDADH configuration, we used the 3NYE crystal structure because it has 100% occupancy of the product[22] and transformed the iminoarginine product to the D-arginine or D-leucine substrate. For both substrate free and substrate-bound models, the isoalloxazine ring was modeled in its oxidized form, which is the state prior to substrate oxidation. Missing hydrogen atoms were added and optimized using the Protein Preparation Wizard[23] in Maestro.[24] *In silico* PaDADH variants with Y249F and Y53F single-point mutations were generated using the Residue Scanning module of BioLuminate[25] for substrate free, D-leucine-bound, and D-arginine-bound configurations. PaDADH binding sites of open configurations were characterized using SiteMap[26] by first calculating the binding site volume as beads placed on a 1 Å grid and determining the local hydrophobic−hydrophilic character.

QM/MM geometry optimizations for all PaDADH models were performed at the B3LYP/6-31G* and B3LYP/cc-pVDZ+ levels of theory, as implemented in QSite.[27] For substrate free models, the QM regions included the Y53(F) and Y249(F) side chains and the isoalloxazine ring of the flavin cofactor (Figure 2a). For substrate-bound configurations, D-leucine/arginine

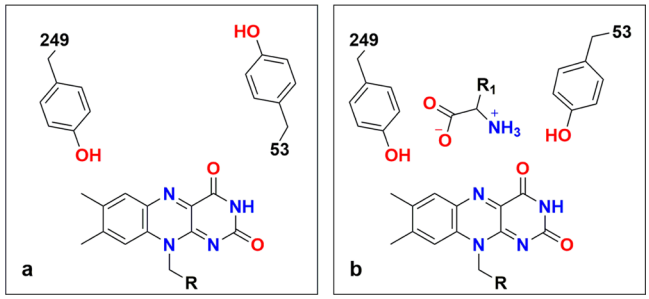

Figure 2. Illustration of the QM region in (a) open, substrate free and (b) closed, substrate-bound configurations. R_1 in panel b denotes the D-leucine and D-arginine side chains. For the sake of simplicity, only wild-type PaDADH is shown.

substrates were also included in the QM region, as illustrated in Figure 2b. The rest of the system was treated using the OPLS2005[28,29] molecular mechanics force field. Local electrophilicity was predicted for the flavin C4a and N5 atoms on the basis of the computed global electrophilicity power of the system and regional Fukui functions. Fukui functions can be used to describe the electron density in frontier atomic orbitals,[30,31] while the global electrophilicity of a system is a quantitative approximation of the likelihood of a system to accept electrons and is calculated as electronegativity squared divided by twice the chemical hardness.[32−34]

Data Analysis. Data were fit with the KaleidaGraph (Synergy Software, Reading, PA), Enzfitter (Biosoft, Cambridge, U.K.), the Kinetic Studio Software Suite (Hi-Tech Scientific, Bradford on Avon, U.K.), or the global-fitting analysis software SPECFIT/32. Time-resolved flavin reductions were fit to eqs 1 and 2, which describe single- and double-exponential processes, respectively, for flavin reduction.

$$A = Be^{-k_{obs}t} + C \quad (1)$$

$$A = B_1e^{-k_{obs1}t} + B_2e^{-k_{obs2}t} + C \quad (2)$$

where k_{obs}, k_{obs1}, and k_{obs2} are the first-order rate constants associated with the absorption changes at 446 nm at a given concentration of the substrate, t is time, A is the absorbance at

dx.doi.org/10.1021/bi500917q | *Biochemistry* 2014, 53, 6574−6583

446 nm at any given time, B, B_1, and B_2 are the amplitudes of the absorption changes, and C is the absorbance at infinite time to account for the non-zero absorbance of the reduced enzyme.

Reductive half-reaction kinetic parameters were determined by using eqs 3 and 4, which describe hyperbolic trends with and without a y-intercept.

$$k_{obs} = \frac{k_{red}S}{^{app}K_d + S} + k_{rev} \quad (3)$$

$$k_{obs} = \frac{k_{red}S}{^{app}K_d + S} \quad (4)$$

where k_{obs} is the observed first-order rate constant for the reduction of the flavin at any given concentration of substrate (S), k_{red} is the limiting first-order rate constant for flavin reduction at saturating substrate concentrations, k_{rev} is the limiting first-order rate constant for the reverse of flavin reduction, and $^{app}K_d$ is the apparent equilibrium constant for dissociation of the enzyme−substrate complex into free enzyme and substrate.

Substrate deuterium KIEs were calculated using eq 5, which applies for a KIE on the k_{red} value. Solvent and multiple deuterium KIEs were calculated using eq 6, which describes a KIE on the k_{red} value and a solvent effect on the K_d value due to pH.

$$k_{obs} = \frac{k_{red}S}{(K_s + S)[1 + F_i(^{D}k_{red} - 1)]} \quad (5)$$

$$k_{obs} = (k_{red}S)/\{K_d[1 + F_i(^{D}k_{red}/^{SE}K_d) - 1] + S[1 + F_i(^{D}k_{red} - 1)]\} \quad (6)$$

where F_i represents the fraction of heavy atom, $^{D}k_{red}$ is the KIE on k_{red}, and $^{SE}K_d$ is the solvent effect due to pH on the apparent K_d value elicited by substituting H_2O with D_2O at those pL values where K_d is not pH-independent.[13]

The pH dependences of the k_{red} values were fit using eq 7

$$\log k_{red} = \log\left[\frac{k_{red(lim)}}{1 + 10^{pK_a - pH}}\right] \quad (7)$$

where $k_{red(lim)}$ represents the pH-independent limiting value for flavin reduction at high pH and pK_a is the apparent value for the ionization of a group that must be unprotonated for flavin reduction.

The pH dependence of the k_{rev} value with the Y53F enzyme was fit using eq 8 describing a curve with two plateau regions

$$\log k_{rev} = \log\left[\frac{k_{rev(L)} + k_{rev(H)} \times 10^{pH - pK_a}}{1 + 10^{pH - pK_a}}\right] \quad (8)$$

where $k_{rev(L)}$ and $k_{rev(H)}$ indicate lower and higher limiting values at low and high pH, respectively, and K_a is the dissociation constant of the ionizable groups.

The pH dependences of the K_d values were fit using eq 9, which describes a curve with a slope of +1 at high pH and a plateau region that defines a limiting, pH-independent K_d value at low pH, i.e., $K_{d(lim)}$.

$$\log K_d = \log[K_{d(lim)}(1 + 10^{pH - pK_a})] \quad (9)$$

RESULTS

Purification of the Y53F and Y249F Enzymes. Y53 and Y249 of PaDADH were mutated to phenylalanine using site-directed mutagenesis, and the resulting proteins were expressed and purified to high levels following the same procedure previously used for the wild-type enzyme.[14] The Y53F enzyme exhibited a UV−visible absorption spectrum similar to that of the wild-type enzyme (Figure 3), whereas the Y249F variant

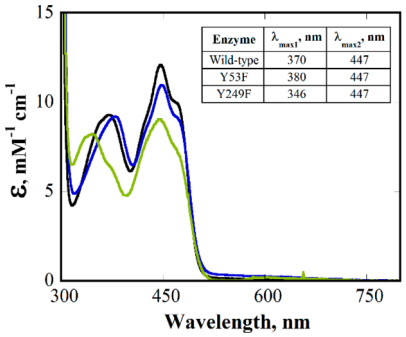

Figure 3. UV−visible absorption spectra of Y53F (blue), Y249F (green), and wild-type (black) PaDADH in 20 mM Tris-HCl and 10% glycerol (pH 8.7) at 22 °C.

was present in two forms that could be separated on a DEAE-Sepharose column: a yellow fraction containing FAD (Figure 3) and a green fraction containing a modified form of FAD (S. Gannavaram and G. Gadda, unpublished observations). The FAD-containing fraction was enzymatically active, whereas the green fraction was inactive with D-arginine or D-leucine as the substrate. No conversion of the yellow fraction to green was observed during enzyme turnover or reductive half-reaction with amino acid substrates (S. Gannavaram and G. Gadda, unpublished observations). Hence, this work focuses on the yellow fraction; the inactive green flavin extracted from the Y249F enzyme has been characterized by nuclear magnetic resonance, mass spectrometry, high-performance liquid chromatography, and UV−visible absorption spectroscopy and will be discussed in future work. Both the Y53F and Y249F enzymes oxidized D-arginine, with steady-state kinetic parameters at 1 mM PMS similar to those of the wild-type enzyme at pH 8.7 (Table 1).

Table 1. Steady-State Kinetic Parameters for Y53F and Y249F Enzymes with D-Arginine[a]

enzyme	$^{app}k_{cat}/K_m$ (M^{-1} s^{-1})	$^{app}K_m$ (mM)	$^{app}k_{cat}$ (s^{-1})
Y53F	$(1.2 \pm 0.1) \times 10^6$	0.36 ± 0.01	420 ± 4
Y249F	$(3.4 \pm 0.3) \times 10^6$	0.06 ± 0.01	204 ± 6
wild-type[b]	$(3.4 \pm 0.3) \times 10^6$	0.06 ± 0.01	204 ± 6

[a]In 20 mM Tris-HCl (pH 8.7) at 25 °C with 0.01−3.0 mM D-arginine and 1 mM PMS. [b]Taken from ref 22.

pH Profiles of k_{red}. The reductive half-reaction with D-arginine in the Y53F and Y249F enzymes was too fast to be studied in a stopped-flow spectrophotometer, with >80% of the flavin being completely reduced within the mixing time of the instrument (i.e., 2.2 ms). This was previously observed in the wild-type enzyme.[14] The reaction was thus investigated with D-leucine as the reducing substrate, for which data for the wild-type enzyme are available to compare and contrast. Flavin reduction was monitored at 446 nm upon mixing PaDADH

dx.doi.org/10.1021/bi500917q | Biochemistry 2014, 53, 6574−6583

(~10 μM) with varying concentrations of D-leucine (≥100 μM) to ensure pseudo-first-order conditions. With the exception of the Y249F enzyme at pH ≥10.0, the stopped-flow traces with both enzyme variants were best fit to single-exponential processes at any pH (Figure 4). At pH ≥10.0, the

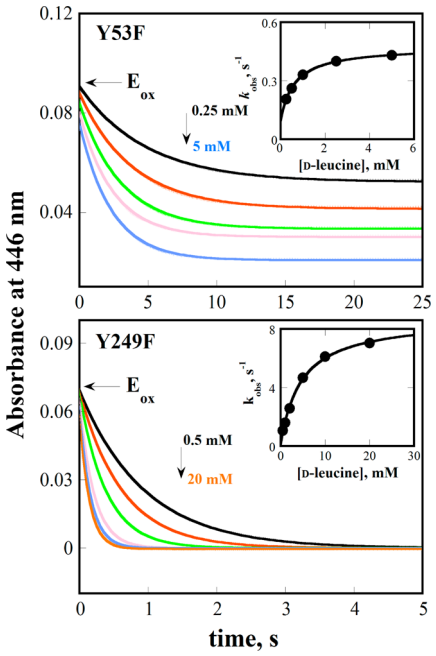

Figure 4. Reductive half-reactions for the Y53F and Y249F enzymes with D-leucine. Stopped-flow traces at 446 nm at varying D-leucine concentrations are shown for Y53F at pH 8.0 (top) and Y249F at pH 9.0 (bottom). E_{ox} is the absorbance of the enzymes in the oxidized state after mixing with buffer. Insets show the concentration dependences of k_{obs} with the best fit of the data points obtained with eqs 3 and 4 for the Y53F and Y249F enzymes, respectively.

Y249F enzyme showed biphasic flavin reduction with a small slow phase independent of D-leucine concentration that accounted for the ~10% absorption change, probably due to partially damaged enzyme originating in the preparation of the enzyme at high pH. With both enzymes, observed rate constants for flavin reduction (k_{obs}) increased hyperbolically with an increasing substrate concentration, defining limiting rate constants for flavin reduction at a saturating concentration of D-leucine (k_{red}) (Figure 4, insets). For the Y53F enzyme, *y*-intercepts significantly different from zero were obtained by fitting the data to eq 3, consistent with reversible flavin reduction (Figure 4, inset).[35] A similar pattern was seen with the Y249F enzyme at pH ≤8.0, whereas the *y*-intercepts with the latter enzyme were negligible at pH ≥8.5 (Figure 4, inset). With both enzymes, the reversibility was more prominent at low pH because of a progressive decrease in the k_{red} values (Figure 5). In contrast, previous results with the wild-type enzyme demonstrated negligible *y*-intercepts in the same pH range from 7.0 to 10.5.[13]

The k_{red} values for the Y53F and Y249F enzymes increased with an increase in pH (Figure 5), defining apparent pK_a values not significantly different from the value of 9.6 previously determined for the wild-type enzyme (Table 2). The estimated pH-independent k_{red} values with both enzyme variants were <3-fold lower than in the wild-type enzyme (Table 2), indicating that neither Y53 nor Y249 is essential for amine oxidation. With the Y53F enzyme, the k_{rev} value increased with an increase in

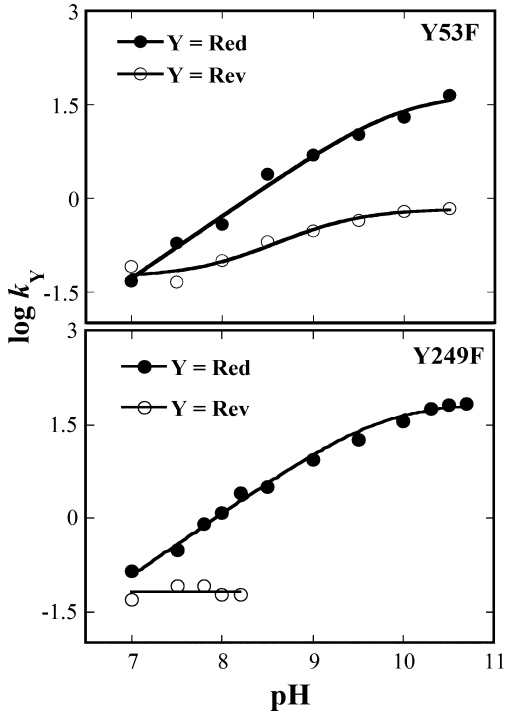

Figure 5. Effects of pH on k_{red} and k_{rev} of the Y53F (top) and Y249F (bottom) enzymes with D-leucine. The k_{red} values (●) were fit with eq 7, whereas the k_{rev} values (○) were fit with eq 8 for the Y53F enzyme. The horizontal line in the plot of the Y249F enzyme is the average of the k_{rev} values.

Table 2. Effects of pH on k_{red} and $^{app}K_d$

enzyme	k_{red} (s^{-1})	pK_a (k_{red})	$^{app}K_d$ (mM)	pK_a (K_d)
Y53F	~50[a]	~10.0[a]	0.5 ± 0.1	9.0 ± 0.1
Y249F	~70[a]	~9.8[a]	3.5 ± 0.3	9.6 ± 0.1
wild-type[b]	133 ± 5	9.6	3.5 ± 0.3	10.3 ± 0.1

[a]Approximate value, as the plateau is not well-defined. [b]Taken from ref 13.

pH between limiting values at low and high pH values of 0.05 ± 0.01 and 0.7 ± 0.1 s^{-1}, respectively, defining a pK_a of 9.1 ± 0.2 (Figure 5). The $^{app}K_d$ values were pH-independent below pH 8.5 and increased with an increasing pH (Figure 6), defining apparent pK_a values slightly lower than in the wild-type enzyme (Table 2). While the pH-independent $^{app}K_d$ for the Y249F

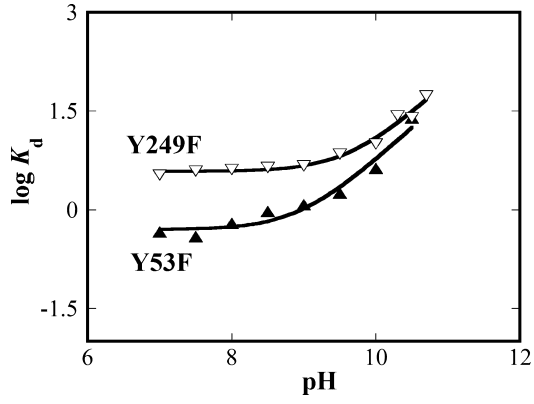

Figure 6. Effects of pH on $^{app}K_d$ values of the Y53F and Y249F enzymes with D-leucine. Data points were fit with eq 9.

dx.doi.org/10.1021/bi500917q | *Biochemistry* 2014, 53, 6574−6583

enzyme was similar to that of the wild type, the value for the Y53F enzyme was 7-fold lower (Table 2).

Substrate Deuterium KIEs on k_{red}. Substrate deuterium KIEs were measured with D-leucine and D-leucine-d_{10} at pL 10.5 to gain insight into the status of the CH bond in the transition state for amine oxidation catalyzed by the Y53F and Y249F enzymes. $^{D}k_{red}$ values of >4 were observed in aqueous buffered solutions with both the Y53F and Y249F enzymes (Table 3).

Table 3. KIEs on k_{red} in the Y53F and Y249F Enzymes[a]

KIE	Y53F	Y249F	wild-type[b]
$^{D}(k_{red})_{H_2O}$	4.2 ± 0.4	4.7 ± 0.1	5.1 ± 0.1
$^{D}(k_{red})_{D_2O}$	5.0 ± 0.2	4.3 ± 0.1	4.7 ± 0.1
$^{D_2O}(k_{red})_{H}$	2.1 ± 0.1	1.3 ± 0.1	1.8 ± 0.1
$^{D_2O}(k_{red})_{D}$	2.3 ± 0.1	1.3 ± 0.1	1.6 ± 0.1
$^{D,D_2O}(k_{red})$	12 ± 2	5.7 ± 0.1	7.8 ± 0.1
$^{D}(k_{red})_{H_2O}{}^{D_2O}(k_{red})_{H}$	9 ± 1	6.1 ± 0.2	9.0 ± 0.2

[a]In 20 mM EDTA (pL 10.5) at 25 °C. [b]From ref 13.

Upon substitution of H_2O with D_2O, the substrate deuterium KIE increased slightly in the Y53F enzyme, whereas it decreased slightly in the Y249F enzyme. The changes, however, were not statistically significant within the associated standard errors (Table 3).

Solvent Deuterium KIEs on k_{red}. Solvent deuterium KIEs were measured at pL 10.5 to probe the status of the substrate NH bond in the transition state for amine oxidation catalyzed by the Y53F and Y249F enzymes. The high pL was chosen because k_{red} is independent of pL in the wild type[13] and the enzyme variants (Table 2), thereby eliminating possible artifactual effects due to different ionizations of relevant groups in H_2O and D_2O. The data were fit to eq 6, which allows for the determination of the $^{D_2O}k_{red}$ values while accounting for solvent effects due to pH on the $^{app}K_d$ values, as previously described for wild-type PaDADH.[13] Small but significant $^{D_2O}k_{red}$ values with magnitudes similar to the magnitudes of those of wild-type PaDADH were determined for both mutant enzymes (Table 3). Because D_2O is ~25% more viscous than H_2O, the possibility that the small $^{D_2O}k_{red}$ values could be due to viscosity rather than isotope effects exists. This was assessed by determining the effect of solvent viscosity on the rate constant for flavin reduction in the absence and presence of 10% glycerol, which provides viscosity at 25 °C equivalent to that of D_2O. The solvent viscosity effect on k_{red}, expressed as $k_{red}/k_{red(glycerol)}$, was 1.06 ± 0.04 for the Y53F enzyme and 0.94 ± 0.01 for the Y249F enzyme, consistent with the $^{D_2O}k_{red}$ values solely arising from KIE and not solvent viscosity effects, as previously established for the wild-type enzyme.[13] Substitution of D-leucine with D-leucine-d_{10} resulted in no changes in either the Y53F or the Y249F enzyme (Table 3).

Multiple KIEs on k_{red}. Multiple deuterium isotope effects ($^{D,D_2O}k_{red}$) were determined to dissect the contributions of the hydroxyl groups of Y53 and Y249 to the relative timing of CH and NH bond cleavages in the transition state(s) for amine oxidation catalyzed by the mutant enzymes. The $^{D,D_2O}k_{red}$ values for both Y53F and Y249F enzymes at pL 10.5 are summarized in Table 3. The $^{D,D_2O}k_{red}$ is similar within standard deviation to the product of the individual deuterium isotope effects, $^{D}(k_{red})_{H_2O}{}^{D_2O}(k_{red})_{H}$, for the Y53F and Y249F enzyme variants. In contrast, in the wild-type enzyme, the multiple KIE was slightly lower than the product of the individual ones (Table 3).[13]

Time-Resolved Absorption Spectroscopy. The reductive half-reactions of the Y53F and Y249F enzymes, as well as wild-type PaDADH, were further studied at pH 10.5 in a stopped-flow spectrophotometer equipped with a photodiode array detector to evaluate whether transient intermediates were formed during the oxidation reaction. With D-leucine or D-leucine-d_{10} as a substrate, flavin reduction occurred without transient accumulation of any flavin-derived intermediate, as indicated by the stopped-flow traces at any wavelength between 300 and 700 nm (Figure 7). These results do not allow us to rule out any of the potential mechanisms for amino acid oxidation because flavin adducts that decay faster than they form would not accumulate to detectable levels.

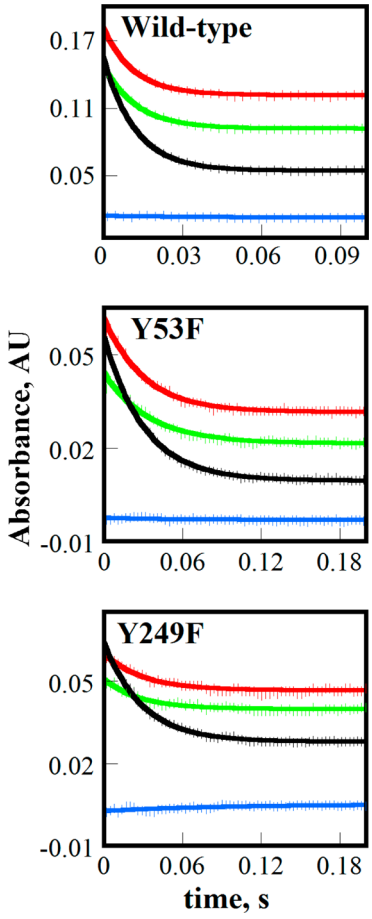

Figure 7. Time-resolved absorbance spectroscopy of wild-type, Y53F, and Y249F PaDADH. D-Leucine was used as a substrate in the stopped-flow spectrophotometer attached to a photodiode array detector. The experiment was conducted in 20 mM EDTA (pH 10.5) at 25 °C. Time courses for changes in absorbance at four different wavelengths are represented in the figure: 371 nm (red), 394 nm (green), 447 nm (black), and 590 nm (blue) for wild-type, Y53F, and Y249F enzymes. All traces in the three enzymes were fit to eq 1, corresponding to a monophasic process. Note that the starting concentration of the FAD cofactor is not the same for the three enzymes.

Relative Electrophilicity of the Flavin C4a and N5 Atoms. The relative electrophilicity of the flavin N5 and C4a atoms is important for distinguishing among the three proposed mechanisms for D-amino acid oxidation catalyzed

dx.doi.org/10.1021/bi500917q | Biochemistry 2014, 53, 6574−6583

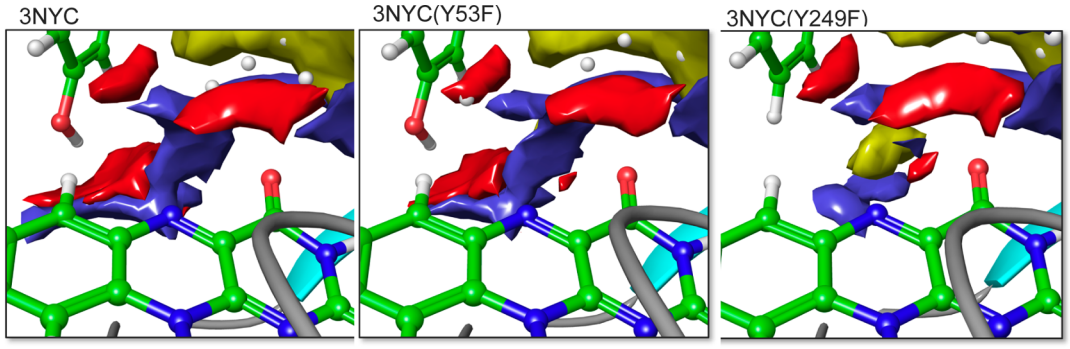

Figure 8. Electrophilicity of the substrate binding sites close to the flavin C4a and N5 atoms in wild-type, Y53F, and Y249F PaDADH. Hydrophilic regions are divided into hydrogen bond donor (blue) and acceptor (red) regions, whereas hydrophobic regions are colored yellow. The white spheres denote SiteMap points that are placed into a 1 Å grid and used to calculate the binding site volume used to evaluate the binding site.

by PaDADH. In the carbanion and hydride transfer mechanisms, the flavin N5 atom is expected to be more electrophilic than the C4a atom, while the opposite is expected for the polar nucleophilic mechanism. The active site of PaDADH was characterized computationally for the wild type and the two enzyme variants without substrate bound in an effort to first reveal possible effects of mutagenesis on the substrate binding site and substrate recognition (Figure 8). The active site cavity was mapped computationally for hydrophilic (blue and red) and hydrophobic (yellow) characteristics as described in Experimental Procedures. The hydrophilic regions were further characterized as hydrogen bond donor and acceptor regions, colored blue and red, respectively. In the substrate free state, the Y249F mutation changes the hydrogen bond donor character near the flavin N5 atom, while the Y53F mutation has little effect on the properties of the cavity near the N5 atom compared to those of the wild-type enzyme. Local electrophilicity indices for the flavin N5 and C4a atoms of PaDADH in the substrate free and substrate bound configurations were then computed after modeling either D-arginine or D-leucine in the active site of the enzyme (Figure 9). This showed that the flavin N5 atom is a better electrophile than the C4a atom and is the preferential site for attack, irrespective of the starting configuration, the presence or absence of a substrate, or the substrate identity (Figure 10). Computational characterization also showed that the electrophilicity of the flavin N5 atom is further increased upon substrate binding as compared to the C4a electrophilicity index.

The computational modeling of the substrates bound in the active site of the enzyme showed that the hydroxyl group of Y249 is 2.7−2.9 Å from one of the carboxyl O atoms of D-arginine or D-leucine (Figure 9), as it was previously inferred form the crystal structures of the iminoarginine− and iminohistidine−enzyme complexes at 1.3 Å resolution. The closest interaction of the hydroxyl group of Y53 with the substrate is, however, with the other carboxyl O atom rather than the α-amine, with a distance of 3.6 Å in both enzyme−substrate complexes (Figure 9). The substrate α-amino group is 3.1−3.9 Å from the flavin O4 atom, whereas the substrate α-proton is between 3.3 and 3.6 Å from the flavin N5 atom (Figure 9).

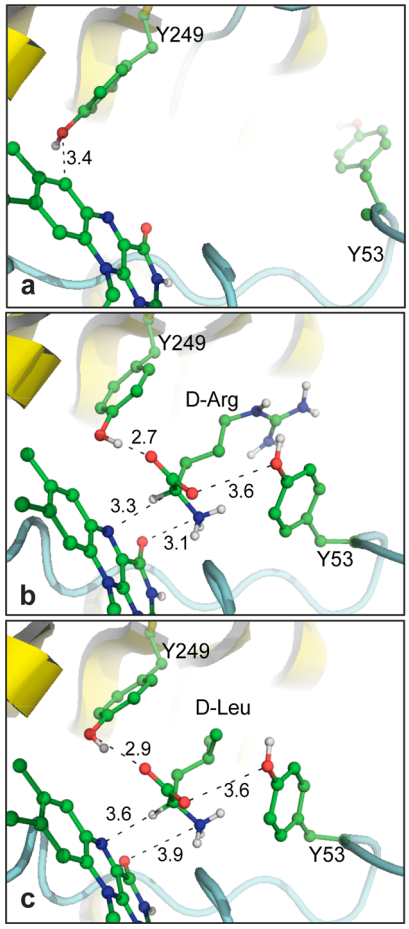

Figure 9. Illustration of wild-type PaDADH structures used to characterize isoalloxazine electrophilicity: (a) open and free, (b) closed and D-arginine-bound, and (c) closed and D-leucine-bound conformations. For the sake of simplicity, only non-hydrogen atom distances among flavin, PaDADH active site residues, and the bound substrates are illustrated.

DISCUSSION

A previous study of the reductive half-reaction of wild-type PaDADH using substrate and solvent KIEs established that the oxidation of D-leucine to the imino product 4-methyl-2-oxopentanoate occurs through the asynchronous cleavages of the substrate NH and CH bonds.[13] Thus, amino acid oxidation could take place via hydride transfer, a carbanion or a polar nucleophilic mechanism (Scheme 2). Here, we have investigated the reductive half-reactions of the Y53F and Y249F variants of PaDADH using substrate and solvent deuterium KIEs, solvent viscosity and pH effects, and QM/MM computational approaches. The mutations were selected

dx.doi.org/10.1021/bi500917q | Biochemistry 2014, 53, 6574−6583

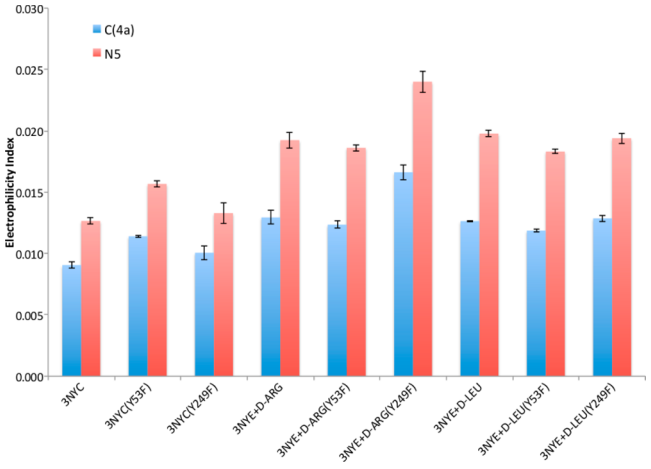

Figure 10. Calculated local electrophilicity centered around C4a and N5 atoms (units of electronvolts). The QM region was described using B3LYP/cc-pVDZ+, while the protein was described using the OLPS2005 force field. The QM region included the isoalloxazine ring of the flavin cofactor and the side chains of amino acids 249 and 53. In addition, D-arginine and D-leucine substrates were included in the QM regions for the models denoted 3NYE+D-ARG and 3NYE+D-LEU, respectively. The mean and standard deviation were determined from three individual QM/MM optimizations, in which the starting structures were perturbed via a restrained minimization using root-mean-square deviation cutoffs of 0, 0.3, and 0.5 Å.

because in the X-ray crystallographic structure of the wild-type enzyme in complex with the reaction product iminoarginine the hydroxyl groups of the two tyrosines are ≤4 Å from the imino and carboxylate moieties of the ligand, suggesting participation in catalysis and binding.[13,22]

The cleavages of the NH and CH bonds of D-leucine catalyzed by the Y53F and Y249F variants of PaDADH occur in synchronous fashion, consistent with a hydride transfer mechanism for flavin reduction. Evidence of a hydride transfer mechanism, in which the substrate amine proton is in flight in the transition state for CH bond cleavage, comes from the multiple deuterium KIEs on the k_{red} value determined with both enzyme variants. In the transition state for amino acid oxidation, substrate deuterium KIEs directly probe the status of the CH bond, whereas solvent deuterium KIEs report on the status of the substrate NH bond. The $^{D}k_{red}$ values are >4 in both enzymes, consistent with CH bond cleavage contributing to the transition state leading to amino acid oxidation. Similarly, $^{D_2O}k_{red}$ values of >1 were determined with both enzyme variants, suggesting that NH bond cleavage also contributes to the transition state for amino acid oxidation. With the Y53F enzyme, the $^{D,D_2O}k_{red}$ obtained with D-leucine in water and D-leucine-d_{10} in D_2O is 12, which is similar to, if not slightly larger than, the product of the individual substrate and solvent deuterium KIEs, with a value of 9. With the Y249F enzyme, the $^{D,D_2O}k_{red}$ is the same as the product of the individual KIEs, i.e., 5.7 versus 6.1. This is consistent with the two bonds probed by the substrate and solvent deuterium KIEs being cleaved in concerted, synchronous fashion.[36] In contrast, a stepwise mechanism in which the two bonds are cleaved in two separate kinetic steps, such as in carbanion and polar nucleophilic mechanisms, is not consistent with the observed results because a multiple-deuterium KIE significantly smaller than the product of the individual deuterium KIEs is expected in this case.[36] Consistent with a hydride transfer mechanism, the QM/MM computations demonstrate that the flavin N5 atom accepting the hydride ion from the amino acid substrate is a better electrophile than the C4a atom, which was proposed to be more reactive in other flavoprotein oxidases, such as monoamine oxidase.[21] Additionally, the computational model of the wild-type enzyme in complex with either D-arginine or D-leucine built from the crystallographic structure of the enzyme−iminoarginine complex shows that the substrate Cα atom is positioned ≤3.6 Å from the flavin N5 atom, in a geometry that is consistent with a hydride transfer mechanism.

Despite Y53 being suitably positioned in the active site of the enzyme to deprotonate the substrate α-amine,[13,22] this residue is not the catalytic base with a pK_a of 9.6 that triggers the hydride transfer reaction to the flavin. Evidence in support of this conclusion comes from the reductive half-reaction determined with D-leucine as the substrate, showing an only <3-fold decrease in the limiting value for k_{red} at high pH in the Y53F enzyme compared to that of the wild type. Although an accurate determination of the pK_a value could not be conducted, the pH profile for k_{red} in the Y53F enzyme demonstrates that an unprotonated group is still required for flavin reduction. These results are consistent with Y53 not being the catalytic base in PaDADH. Similar conclusions are drawn for Y249 based on the results of the rapid reaction studies on the Y249F enzyme, showing a <3-fold decrease in the pH-independent k_{red} value at high pH and the presence of a pK_a similar to that of the wild-type enzyme for an unprotonated group required for catalysis. Thus, site-directed mutagenesis showed that neither tyrosine is responsible for the pK_a of 9.6 in wild-type PaDADH. The computational models of the enzyme in complex with D-arginine and D-leucine are consistent with the mutagenesis because they place the protein hydroxyl groups closest to the carboxyl O atoms of the substrate rather than the substrate α-amino group. Future studies using site-directed mutagenesis will be aimed at evaluating whether H48 is the group acting as a base for amine deprotonation in the active site of PaDADH, having its side chain separated by two intervening water molecules from the α-imine of the reaction product in the crystal structure of the enzyme in complex with iminoarginine.[22]

The side chain hydroxyl of Y249 is not playing a major role in substrate binding in wild-type PaDADH, as previously proposed on the basis of its location in the crystal structure of the enzyme in complex with iminoarginine. Thus, the pK_a of 10.3 seen in the pH profile of the $^{app}K_d$ value previously reported for the wild-type enzyme is assigned to the unbound substrate α-amino group. Evidence for this conclusion comes from the pH profile of the $^{app}K_d$ value determined in a stopped-flow spectrophotometer for the Y249F enzyme, with a pH-independent $^{app}K_d$ value of 3.5 mM that is identical to that of the wild-type enzyme.[13] Replacement of Y249 with phenylalanine results in a shift in the pK_a from 10.3 to 9.6, underlining the importance of establishing pH effects to avoid artifactual contribution of pH when comparing kinetic parameters of mutated and wild-type enzymes.[37] The Y53F enzyme also shows a perturbed pK_a for $^{app}K_d$, with a value of 9.0. If the protonated substrate makes a hydrogen bond with the protein, then the unprotonated substrate could make the same, but weaker, hydrogen bond with the protein. Interestingly, substrate binding in the Y53F variant is 7-fold tighter than in the wild-type enzyme, as indicated by the pH-independent $^{app}K_d$ value of 0.5 mM compared to the value of 3.5 mM at low pH. This may be the result of increased hydrophobic effects

dx.doi.org/10.1021/bi500917q | Biochemistry 2014, 53, 6574−6583

between the benzene moiety of F53 and the hydrophobic side chain of D-leucine.

Conversion of the oxidized enzyme−amino acid complex to the reduced enzyme−imino acid complex in PaDADH becomes reversible upon removing the hydroxyl group from either Y53 or Y249, likely due to a change in the driving force for reversible flavin reduction upon removal of the protein hydroxyls from the active site of the enzyme. This is in contrast to the wild-type enzyme, for which irreversible flavin reduction was previously established.[13] Evidence of reversible flavin reduction comes from the reductive half-reactions of the Y53F and Y249F enzymes with D-leucine at low pH, showing non-zero *y*-intercepts in the plots of the observed rates of flavin reduction (k_{obs}) as a function of substrate concentration. This behavior is observed over a limited pH range in the Y249F enzyme, i.e., 7.0−8.2, with the rate constant for the reverse of the flavin reduction reaction (k_{rev}) becoming negligible compared to k_{red}, and therefore not amenable to measurement, as the pH increases above 8.2. However, with the Y53F enzyme, reversible flavin reduction is observed throughout the pH range from 7.0 to 10.5 used in the experiment, allowing for a mechanistic analysis of the reductive half-reaction in the latter mutant enzyme. A pK_a of 9.1 is seen in the pH profile of k_{rev} for the Y53F enzyme, which is assigned to the ionization of the flavin N1 atom in the reduced enzyme in the reverse amino acid oxidation reaction. For comparison, N1 of reduced FMN has pK_a values between 5.8 and 7.0 when it is bound to flavodoxin from *Megaspahera elsdenii* or *Desulfovibrio vulgaris*[39] and 6.7 when it is free in solution,[40] as previously established through optical or redox determinations. Reversible flavin reduction in the oxidation of amino acids was previously reported in D-amino acid oxidase from *Trigonopsis variabilis* using para-substituted phenylglycine substrates and glycine oxidase from *Bacillus subtilis* with proline as the substrate.[3,38]

In summary, through the use of mechanistic and computational approaches and site-directed mutagenesis, we have demonstrated that the FAD-mediated oxidation of the substrate CN bond in PaDADH lacking protein hydroxyls in the active site occurs via hydride transfer. The enzyme variants engineered through mutagenesis of Y53 and Y249 to phenylalanine stabilize transition states for amino acid oxidation in which the substrate NH and CH bonds are cleaved in synchronous fashion. In contrast, the transition state is asynchronous in the wild-type enzyme, as previously reported.[13] These observations can be accommodated with PaDADH utilizing a hydride transfer mechanism for catalysis, with the relative timing for NH and CH bond cleavage being altered upon removal of the protein hydroxyls interacting with the substrate. If this were the case, one would expect minimal changes in the catalytic properties of the enzyme upon replacement of tyrosine with phenylalanine residues in the active site of the enzyme, as observed when comparing the k_{red}, $^{app}K_d$, $^{D}k_{red}$, and $^{D_2O}k_{red}$ values, as well as the pH profiles for k_{red} and $^{app}K_d$ of the Y53F and Y249F variants with the wild-type enzyme. Both carbanion and nucleophilic mechanisms are more difficult to reconcile with the results of the variant and wild-type enzymes because one would have to assume that the removal of either protein hydroxyl group would cause a dramatic change in the mechanism of the reaction, i.e., involving a flavin N5- or C4a-adduct in the wild-type PaDADH and a hydride transfer mechanism in the Y53F and Y249F enzyme variants, while maintaining minimal changes in the catalytic properties of the variant and wild-type enzyme. A similar conclusion was proposed for flavocytochrome b_2, based on mutagenesis and mechanistic studies using deuterium KIEs.[41] Hydride transfer mechanisms have been recently discussed for D-amino acid oxidase and sarcosine oxidase,[1] which belong to the same structural family of D-arginine dehydrogenases. Thus, as more studies using mutagenesis, kinetic, structural, and computational approaches are conducted, evidence in favor of hydride transfer as the most likely mechanism for amino acid oxidation by flavoproteins is accumulating. PaDADH is further emerging as a model system along with the well-characterized D-amino acid oxidase[1,7] for the study of flavin-dependent amino acid oxidation, as evidenced by the mechanistic and structural data from this study and previous studies.[13,14,22]

AUTHOR INFORMATION

Corresponding Author

*Department of Chemistry, Georgia State University, P.O. Box 3695, Atlanta, GA 30302-3695. E-mail: ggadda@gsu.edu. Phone: (404) 413-5537. Fax: (404) 413-5505.

Funding

This work was supported in part by National Science Foundation Grant MCB-1121695 (to G.G.) and a Molecular Basis of Disease Graduate Fellowship from Georgia State University (to S.G.). Schrödinger, LLC, is the employer of S.S. and funded the computational study.

Notes

The authors declare no competing financial interest.

ACKNOWLEDGMENTS

We thank Lydia Law for the preparation of the Y249F mutant of PaDADH and Dr. Dale Edmondson, Dr. Elvira Romero, and Jacob Ball for critical reading of the manuscript. We thank Schrödinger, LLC, for providing computational resources.

REFERENCES

(1) Fitzpatrick, P. F. (2010) Oxidation of amines by flavoproteins. *Arch. Biochem. Biophys. 493*, 13−25.

(2) Ilari, A., Bonamore, A., Franceschini, S., Fiorillo, A., Boffi, A., and Colotti, G. (2008) The X-ray structure of N-methyltryptophan oxidase reveals the structural determinants of substrate specificity. *Proteins 71*, 2065−2075.

(3) Job, V., Marcone, G. L., Pilone, M. S., and Pollegioni, L. (2002) Glycine oxidase from *Bacillus subtilis*. Characterization of a new flavoprotein. *J. Biol. Chem. 277*, 6985−6993.

(4) Khanna, P., and Schuman Jorns, M. (2001) Characterization of the FAD-containing N-methyltryptophan oxidase from *Escherichia coli*. *Biochemistry 40*, 1441−1450.

(5) Leys, D., Basran, J., and Scrutton, N. S. (2003) Channelling and formation of 'active' formaldehyde in dimethylglycine oxidase. *EMBO J. 22*, 4038−4048.

(6) Trickey, P., Wagner, M. A., Jorns, M. S., and Mathews, F. S. (1999) Monomeric sarcosine oxidase: Structure of a covalently flavinylated amine oxidizing enzyme. *Structure 7*, 331−345.

(7) Mattevi, A., Vanoni, M. A., Todone, F., Rizzi, M., Teplyakov, A., Coda, A., Bolognesi, M., and Curti, B. (1996) Crystal structure of D-amino acid oxidase: A case of active site mirror-image convergent evolution with flavocytochrome b2. *Proc. Natl. Acad. Sci. U.S.A. 93*, 7496−7501.

(8) Li, C., and Lu, C.-D. (2009) Arginine racemization by coupled catabolic and anabolic dehydrogenases. *Proc. Natl. Acad. Sci. U.S.A. 106*, 906−911.

(9) Li, C., Yao, X., and Lu, C. D. (2010) Regulation of the dauBAR operon and characterization of D-amino acid dehydrogenase DauA in

arginine and lysine catabolism of *Pseudomonas aeruginosa* PAO1. *Microbiology 156*, 60−71.
(10) Yoshimura, T., and Esak, N. (2003) Amino acid racemases: Functions and mechanisms. *J. Biosci. Bioeng. 96*, 103−109.
(11) Lu, C. D. (2006) Pathways and regulation of bacterial arginine metabolism and perspectives for obtaining arginine overproducing strains. *Appl. Microbiol. Biotechnol. 70*, 261−272.
(12) Morris, S. M. (2004) Enzymes of Arginine Metabolism. *J. Nutr. 134*, 2743S−2747S.
(13) Yuan, H., Xin, Y., Hamelberg, D., and Gadda, G. (2011) Insights on the mechanism of amine oxidation catalyzed by D-arginine dehydrogenase through pH and kinetic isotope effects. *J. Am. Chem. Soc. 133*, 18957−18965.
(14) Yuan, H., Fu, G., Brooks, P. T., Weber, I., and Gadda, G. (2010) Steady-state kinetic mechanism and reductive half-reaction of D-arginine dehydrogenase from *Pseudomonas aeruginosa*. *Biochemistry 49*, 9542−9550.
(15) Stroud, E. D., Fife, D. J., and Smith, G. G. (1983) A method for the determination of the pK_a of the α-hydrogen in amino acids using racemization and exchange studies. *J. Org. Chem. 48*, 5368−5369.
(16) Porter, D. J. T., Voet, J. G., and Bright, H. J. (1973) Direct Evidence for Carbanions and Covalent N5-Flavin-Carbanion Adducts as Catalytic Intermediates in the Oxidation of Nitroethane by D-Amino Acid Oxidase. *J. Biol. Chem. 248*, 4400−4416.
(17) Gadda, G., Edmondson, R. D., Russell, D. H., and Fitzpatrick, P. F. (1997) Identification of the naturally occurring flavin of nitroalkane oxidase from *Fusarium oxysporum* as a 5-nitrobutyl-FAD and conversion of the enzyme to the active FAD-containing form. *J. Biol. Chem. 272*, 5563−5570.
(18) Hamilton, G. A., and Brown, L. E. (1970) Model reactions and a general mechanism for flavoenzyme-catalyzed dehydrogenations. *J. Am. Chem. Soc. 92*, 7225−7227.
(19) Walsh, C. T., Krodel, E., Massey, V., and Abeles, R. H. (1973) Studies on the Elimination Reaction of D-Amino Acid Oxidase with α-Amino-β-chlorobutyrate: Further Evidence for Abstraction of Substrate α-Hydrogen as a Proton. *J. Biol. Chem. 248*, 1946−1955.
(20) Walsh, C. T., Schonbrunn, A., and Abeles, R. H. (1971) Studies on the mechanism of action of D-amino acid oxidase. Evidence for removal of substrate α-hydrogen as a proton. *J. Biol. Chem. 246*, 6855−6866.
(21) Edmondson, D. E., Mattevi, A., Binda, C., Li, M., Hubálek, F., and Abraham, D. J. (2003) Structure and Mechanism of Monoamine Oxidase. In *Burger's Medicinal Chemistry and Drug Discovery*, John Wiley & Sons, Inc., New York.
(22) Fu, G., Yuan, H., Li, C., Lu, C. D., Gadda, G., and Weber, I. T. (2010) Conformational changes and substrate recognition in *Pseudomonas aeruginosa* D-arginine dehydrogenase. *Biochemistry 49*, 8535−8545.
(23) Sastry, G. M., Inakollu, V. S., and Sherman, W. (2013) Boosting virtual screening enrichments with data fusion: Coalescing hits from 2D fingerprints, shape, and docking. *J. Chem. Inf. Model. 53*, 1531−1542.
(24) *Maestro*, version 9.6 (2013) Schrödinger, LLC, New York.
(25) *BioLuminate*, version 1.1 (2013) Schrödinger, LLC, New York.
(26) *SiteMap*, version 2.9 (2013) Schrödinger, LLC, New York.
(27) *QSite*, version 6.1 (2013) Schrödinger, LLC, New York.
(28) Jorgensen, W. L., and Tirado-Rives, J. (1988) The OPLS [optimized potentials for liquid simulations] potential functions for proteins, energy minimizations for crystals of cyclic peptides and crambin. *J. Am. Chem. Soc. 110*, 1657−1666.
(29) Kaminski, G. A., Friesner, R. A., Tirado-Rives, J., and Jorgensen, W. L. (2001) Evaluation and reparametrization of the OPLS-AA force field for proteins via comparison with accurate quantum chemical calculations on peptides. *J. Phys. Chem. B 105*, 6474−6487.
(30) Parr, R. G., Szentpály, L. v., and Liu, S. (1999) Electrophilicity index. *J. Am. Chem. Soc. 121*, 1922−1924.
(31) Domingo, L. R., Aurell, M. J., Pérez, P., and Contreras, R. (2002) Quantitative characterization of the local electrophilicity of organic molecules. Understanding the regioselectivity on Diels-Alder reactions. *J. Phys. Chem. A 106*, 6871−6875.
(32) Ayers, P. W., and Parr, R. G. (2000) Variational principles for describing chemical reactions: The Fukui function and chemical hardness revisited. *J. Am. Chem. Soc. 122*, 2010−2018.
(33) Chattaraj, P. K., and Parr, R. G. (1993) Density functional theory of chemical hardness. In *Chemical Hardness*, pp 11−25, Springer, Berlin.
(34) Pearson, R. G. (1986) Absolute electronegativity and hardness correlated with molecular orbital theory. *Proc. Natl. Acad. Sci. U.S.A. 83*, 8440−8441.
(35) Strickland, S., Palmer, G., and Massey, V. (1975) Determination of dissociation constants and specific rate constants of enzyme-substrate (or protein-ligand) interactions from rapid reaction kinetic data. *J. Biol. Chem. 250*, 4048−4052.
(36) Cleland, W. W. (1982) Use of isotope effects to elucidate enzyme mechanisms. *CRC Crit. Rev. Biochem. 13*, 385−428.
(37) Edmondson, D. E., and Gadda, G. (2008) Guidelines for the Functional Analysis of Engineered and Mutant Enzymes. In *Protein Engineering Handbook*, pp 1−13, Wiley-VCH Verlag GmbH & Co. KGaA, Berlin.
(38) Pollegioni, L., Blodig, W., and Ghisla, S. (1997) On the mechanism of D-amino acid oxidase. Structure/linear free energy correlations and deuterium kinetic isotope effects using substituted phenylglycines. *J. Biol. Chem. 272*, 4924−4934.
(39) Yalloway, G. N., Mayhew, S. G., Malthouse, J. P., Gallagher, M. E., and Curley, G. P. (1999) pH-dependent spectroscopic changes associated with the hydroquinone of FMN in flavodoxins. *Biochemistry 38*, 3753−3762.
(40) Draper, R. D., and Ingraham, L. L. (1968) A potentiometric study of the flavin semiquinone equilibrium. *Arch. Biochem. Biophys. 125*, 802−808.
(41) Sobrado, P., and Fitzpatrick, P. F. (2003) Solvent and primary deuterium isotope effects show that lactate CH and OH bond cleavages are concerted in Y254F flavocytochrome b2, consistent with a hydride transfer mechanism. *Biochemistry 42*, 15208−15214.